Thin Solid Films 548 (2013) 632–635

Contents lists available at ScienceDirect

Thin Solid Films

journal homepage: www.elsevier.com/locate/tsf

Electrochemical explanation for asymmetric electrowetting response

Mehdi Khodayari, Nathan B. Crane *, Alex A. Volinsky

Department of Mechanical Engineering, University of South Florida, Tampa, FL 33620, USA

ARTICLE INFO

Article history:
Received 10 April 2013
Received in revised form 2 October 2013
Accepted 3 October 2013
Available online 11 October 2013

Keywords:
Electrowetting
Contact angle
Young Lippman
Passivation
Asymmetry

ABSTRACT

In electrowetting, a droplet/substrate contact angle is modulated by applying a potential difference between the droplet and the substrate. Typically, the droplet potential is changed via an auxiliary electrode dipped in the droplet. Here, it is shown that electrochemical reactions lead to a potential drop on the auxiliary electrode in electrowetting, which degrades the droplet contact angle modulation. The magnitude of this effect depends on the voltage polarity. This problem can be addressed by using a dielectric layer, such as SiO_2, which can prevent electrochemical reactions with the electrowetting substrate and the auxiliary electrode.

1. Introduction

Electrowetting on dielectric (EWOD) is an electromechanical process, in which a droplet apparent contact angle changes by applying a voltage between the droplet and the substrate underneath [1]. It has found applications in lenses [2], screens [3], energy harvesting [4], and lab-on-a-chip devices [5–8]. Devices consist of a conductive layer, a single or stacked dielectric layer, and typically, a hydrophobic layer (the hydrophobic layer could also act as a dielectric layer). Typically, the droplet voltage is changed via an auxiliary electrode, which is placed in the droplet, as shown in Fig. 1.

In EWOD, contact angle varies with voltage, following the Lippman equation [9]:

$$\cos\theta_1 = \cos\theta_0 + \varepsilon_0 \cdot \varepsilon_r \cdot V_{source}^2/2 \cdot \delta \cdot \gamma_{LO} \quad (1)$$

Here, θ_0 and θ_1 are the initial and actuated contact angles, V_{source} is the power source voltage, γ_{LO} is the interfacial energy between the droplet and the second phase (here, air), δ and $\varepsilon_0\varepsilon_r$ are the dielectric thickness and permittivity, respectively. Droplet angle decreases with voltage following the Lippman equation. However, the droplet modulation ceases at a certain voltage, which is referred to as the saturation voltage, and the corresponding angle is the saturation angle [9]. Saturation angle is often between 60° and 70° [10]. Typically, saturation angle is independent of the droplet voltage polarity. However, it has been shown that the saturation angle can vary with voltage polarity [11]. Such voltage polarity-dependent saturation angle appears with the use of thin hydrophobic dielectric layers, which has been attributed to the susceptibility of thin dielectrics to adsorb negative ions [11]. Here, another cause is introduced, based on a potential drop on the auxiliary electrode. Electrochemical reactions on the electrowetting substrate are followed by counter reactions on the auxiliary electrode, introducing a potential drop in the auxiliary electrode. It is shown that for anodic polarizations of the droplet the auxiliary electrode potential drop increases, attributed to fast cathodic reactions on the substrate. When a high resistance substrate, such as thermally grown SiO_2 [12] or electrochemically grown Al_2O_3 [13] is used, saturation angle is independent of the droplet voltage polarity, and symmetric electrowetting behavior is observed. This symmetry is attributed to the prevention of electrochemical reactions. We use a stack dielectric layer of SiO_2/Cytop to prevent the electrochemical reactions and to demonstrate symmetric electrowetting. Cytop is a perfluoropolymer from Asahi Glass Co. formulated for spin-coating.

In addition to symmetric electrowetting, the prevention of electrochemical reactions also leads to reliable electrowetting. Here, electrowetting reliability with the SiO_2 substrates is also demonstrated, which is another advantage of the SiO_2 substrates. Two electrolyte solutions, namely 0.1 M NaCl and 0.1 M citric acid are used. Some degradation in droplet modulation is observed over 10,000 trials with 0.1 M NaCl electrolyte solution, while with 0.1 M citric acid, the droplet modulation is quite consistent.

2. Discussion

Upon electric field application, electrolytes diffuse through the dielectric, accompanied by electrochemical reactions [14]. In this study, hydrophobic Cytop with a nominal dielectric constant of 2.1 is used. During electrowetting, electrochemical reactions occur at Cytop defects. This affects EWOD behavior differently, depending on the droplet potential polarity with respect to the wafer (cathodic

* Corresponding author at: 4200 E. Fowler Ave ENB 118, Tampa, FL 33620, USA.
E-mail address: ncrane@usf.edu (N.B. Crane).

0040-6090/$ – see front matter © 2013 Elsevier B.V. All rights reserved.
http://dx.doi.org/10.1016/j.tsf.2013.10.011

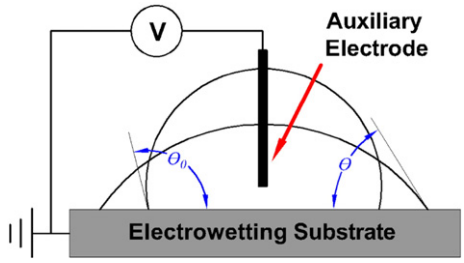

Fig. 1. Schematic of a conventional electrowetting setup. In this process, an electric potential difference is applied between the droplet and the substrate, upon which the droplet/substrate contact angle changes. The droplet potential is changed via an auxiliary electrode. In this study, a platinum wire (0.051 mm diameter, 99.95% pure) is used as the auxiliary electrode.

and anodic reactions occur when the droplet potential is either positive or negative, respectively).

Cathodic reactions continue at high rates, create bubbles, and cause a potential difference between the droplet/substrate interface and the auxiliary electrode due to a potential drop on the auxiliary electrode. The wafer, droplet, and auxiliary electrode potentials were directly measured by adding a platinum reference electrode, as shown in Fig. 2a. In these tests, two electrowetting substrates of Si/SiO_2(500 nm)/Al(300 nm)/Cytop(74 ± 3 nm) were used and the electrical connection was made to the aluminum layer. On each substrate two measurements were performed.

As seen in Fig. 2a, the potential distribution between the wafer and the auxiliary electrode varies with the polarity of the droplet potential. In these tests a passivating system (aluminum/0.1 M citric acid) is used [15]. In passivating systems, the substrate passivates at negative voltage of the droplet, which suppresses electrochemical reactions in the substrate. The substrate passivation is attributed to a barrier-like

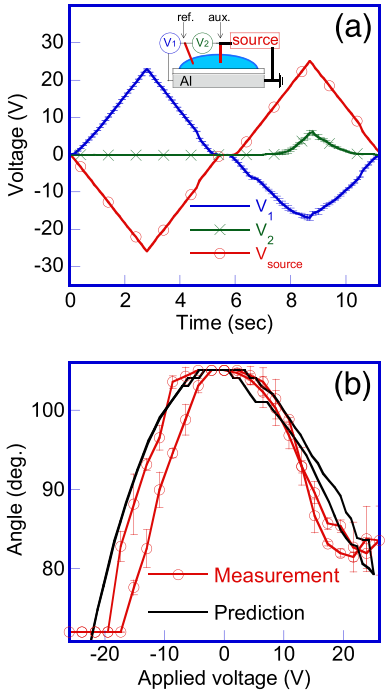

Fig. 2. (a) Direct measurement of the wafer and auxiliary electrode potentials. Reference and auxiliary electrodes are platinum. V_{source}, V_1, and V_2 are the power source voltage, potential drop on the wafer, and potential drop on the auxiliary electrode, respectively; (b) effect of V_1 deviation on the contact angle variation in EWOD. The contact angle values used in Fig. 2b were collected concurrently with the test in Fig. 2a. Contact angles are also predicted with the Lippman equation with V_{source} (dashed line) and V_1 (solid line—the average of V_1 curves obtained on the four spots on two wafers, as shown in Fig. 2a) is used for contact angle prediction. Two aluminum wafers with 74 ± 3 nm Cytop were used, and two tests were performed on each wafer.

alumina (aluminum oxide) formation upon the aluminum oxidation, which impedes the electrolyte diffusion. Alumina is created upon the following reaction [16]:

$$Al + 3H_2O \rightarrow Al_2O_3 + 3H_2 \quad (1)$$

It is noteworthy that in non-passivating systems the same reaction results in alumina formation. However, alumina layer is porous in non-passivating systems, so that it does not prevent continued oxidation, which can damage the aluminum electrode. In this study, a passivating system is used because electrochemical reactions can be either triggered or prevented, depending on the droplet potential polarity. Hence, the effects of the presence and absence of electrochemical reactions on the contact angle variation can be investigated in one measurement.

At positive voltages of the droplet, water hydrolysis occurs in the substrate and the auxiliary electrode as follows: in the substrate (cathodic reaction):

$$2H^+(aq) + 2e^- \rightarrow H_2(g) \quad (2)$$

in the auxiliary electrode (anodic reaction):

$$2H_2O(l) \rightarrow O_2(g) + 4H^+(aq) + 4e^- \quad (3)$$

Here, the auxiliary electrode is platinum, which is a noble metal, immune to oxidation. Therefore, water hydrolysis is the most feasible electrochemical reaction in the auxiliary electrode, which results in oxygen bubble formation. The droplet images at negative and positive voltages of a 0.1 M citric acid droplet on the aluminum wafer are shown in Fig. 3a, b and c. Fig. 3b shows how oxygen bubbles start to form at around +15 V and Fig. 3c shows how their number increases at higher voltages. Typically, some oxygen bubbles depart from the auxiliary electrode, move up, and are released to air at the droplet/air interface, while there is always a population of oxygen bubbles on the auxiliary electrode.

Upon electrochemical reaction commencement, bubbles on the auxiliary electrode narrow the paths for the diffusion of hydrogen cations and oxygen molecules from the auxiliary electrode to the droplet. Therefore, the concentration and electrochemical potential of the hydrogen cations and oxygen molecules in the vicinity of the auxiliary electrode are increased, which results in an increase in the charge transfer resistance in the auxiliary electrode. Additionally, the bubble accumulation impedes the ion transfer in the liquid next to the auxiliary electrode, which could also cause a potential drop in the vicinity of the auxiliary electrode. These two reasons cause a potential drop at the auxiliary electrode (as shown in Fig. 2a), as well as the dielectric-coated substrate.

Lippman equation can show the impact of the auxiliary electrode potential drop on the actuation angle by replacing V_{source} with V_1:

$$\cos\theta_1 = \cos\theta_0 + \varepsilon_0.\varepsilon.V_1^2/2\delta.\gamma_{LO}. \quad (4)$$

Here, $V_1 = V_{source} - V_2$, and is equal to the electrical potential difference between the wafer and the reference electrode, as shown in Fig. 2a. V_{source} is the power source voltage and V_2 is the potential drop at the auxiliary electrode. V_2 increases with the charge transfer resistance on the auxiliary electrode, which creates a difference between V_1 and V_{source}.

When V_{source} tends towards negative values, the electrochemical reactions on the auxiliary electrode and also V_2 magnitude are insignificant because of the reduction of electrochemical reactions due to substrate passivation. In this case, V_1 is equal to V_{source}, and hence Lippman theory predicts EWOD behavior, so either V_{source} or V_1 is used in Eq. (2).

However, when V_{source} becomes positive, V_2 increases. Therefore, V_1 becomes less than V_{source} and EWOD contact angle behavior can be

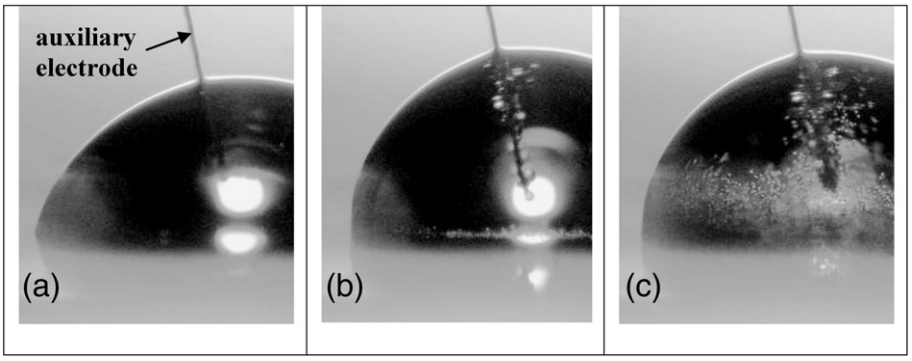

Fig. 3. EWOD on an aluminum wafer with 74 ± 3 nm Cytop when droplet is at (a) −21 V, (b) +15 V, and (c) +21 V.

predicted only if V_1 is used in the Lippman equation. Fig. 2b shows the V_1 deviation effect on the contact angle variation. The Lippman equation predictions with V_1 (V_1 pred.) are also shown (a dielectric thickness of 74 nm, and a droplet surface tension of 72 mN/m have been used in the Lippman equation). The contact angle prediction with V_1 correlates with the contact angle measurements, which substantiates the auxiliary electrode contribution to the contact angle modulation.

The potential drop between the auxiliary electrode and the wafer can be prevented by using a dielectric layer that prevents electrochemical reactions. To achieve this, Cytop was spin-coated over thermally grown SiO_2 on silicon wafers. The electrical connection was made to the silicon layer, below SiO_2. The corresponding wafer and the auxiliary electrode potential variations are shown in Fig. 4a. Two measurements were performed on two substrates. For the angle prediction with the Lippman equation, a dielectric thickness of 151 nm and a dielectric constant of 3.03 were used for the SiO_2 (100 nm)/Cytop (51 ± 4 nm) stack.

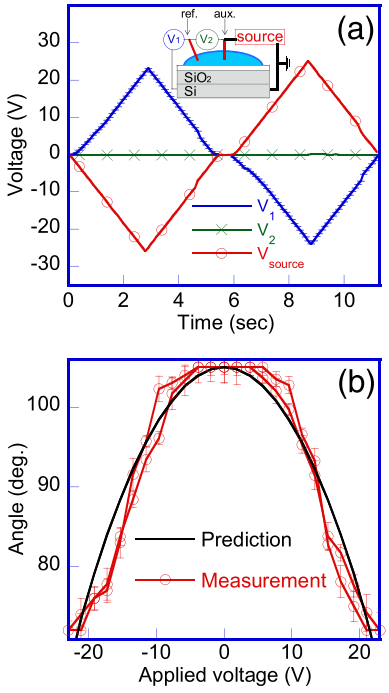

Fig. 4. (a) Potential distribution with an SiO_2 wafer. A 51 ± 4 nm Cytop layer was coated on 100 nm SiO_2 thermally grown on a silicon wafer; (b) Symmetric contact angle variation with an SiO_2 layer without potential distribution between the substrate and the auxiliary electrode.

To calculate SiO_2/Cytop dielectric constant, an equation for two capacitors in series was used as follows:

$$\frac{d_t}{\varepsilon_t} = \frac{d_{cytop}}{\varepsilon_{cytop}} + \frac{d_{sio_2}}{\varepsilon_{sio_2}}. \tag{5}$$

Here, d_t, d_{cytop}, and d_{sio2} are respectively, the total thickness, the Cytop thickness, and SiO_2 thickness. The ε_t, ε_{cytop}, and ε_{sio2} are the total, Cytop, and SiO_2 dielectric constants. For $d_t = 151$ nm, $d_{cytop} = 51$ nm, $d_{sio2} = 100$ nm, $\varepsilon_{cytop} = 2.1$, and $\varepsilon_{sio2} = 3.9$, while ε_t is equal to 3.024. With thermal SiO_2, contact angle varies symmetrically with voltage, as shown in Fig. 4b and V_2 varies between −0.09 V and +0.06 V.

Si/SiO_2/Cytop substrate also provides reliable electrowetting. A challenge in EWOD is to achieve a reliable process. Reliable EWOD can be obtained in passivating systems by preventing electrochemical reactions [17,18]. However, in passivating systems, due to the diode-like behavior of alumina, reliable electrowetting holds only on anodic polarization of the wafer. This limits the EWOD applications, where both potential polarities of the wafer are desired. With a Cytop/SiO_2 composite layer, however, lifelong electrowetting can be achieved with both polarities of the wafer, with insignificant change in the initial and actuation angles. To demonstrate the reliability of the electrowetting systems with SiO_2, the reliability tests were performed for over 10,000 trials with 0.1 M citric acid and 0.1 M NaCl electrolyte solutions in air. In these tests, in each trial, the droplet voltage is switched between 0 V and 37 V (37 V was applied to achieve an initial contact angle near 75°) and is kept at each voltage for 50 ms, while the droplet images are taken in the middle of each voltage application.

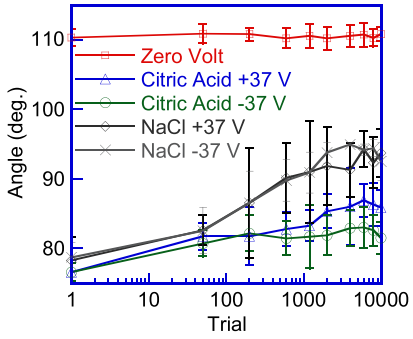

Fig. 5. Demonstration of the electrowetting process. 37 V was applied to obtain a contact angle around 75°. The reliability tests were performed on two similar substrates (Si/SiO2 (500 nm)/Cytop (51 ± 4 nm)) and two spots on each wafer over 10,000 trials. The curves show average contact angles from the four spots and the error bars show the standard deviation. The zero voltage curve shows the average of all measured contact angles (of all tests) and the error bars represent the corresponding standard deviation.

The results are shown in Fig. 5. The reliability tests were performed on two substrates and two spots on each wafer over 10,000 trials. The curves show average contact angles of the four spots. The zero voltage curve shows the average of all measured contact angles.

Here, 51 ± 4 nm Cytop layers were spin coated on two 500 nm SiO_2 wafers (SiO_2 layers were thermally grown on silicon wafers). Then the coated wafers were pre-baked at 100 °C for 90 s and post-baked at 200 °C for 1 h.

As shown in Fig. 5, the droplet actuation does not fail, even though degradation in the contact angle modulation is obvious for all conditions. The contact angle degradation is the least with citric acid when +37 V is applied. The observed reliability is attributed to the high resistivity of the SiO_2 dielectric against electrolyte diffusion, which prevents electrochemical reactions. However, the degradation in the contact angle modulation is attributed to the hydration of SiO_2 dielectric, which can degrade the dielectric properties of SiO_2. It is known that in aqueous medium the surface silicon atoms become saturated by bonding with hydroxyl groups and forming silanol groups (i.e. $\equiv Si-OH$) [19]. However, the structure of the silicon surface can be manipulated by the use of appropriate chemical compounds [19,20]. Our speculation is that with citric acid the reactions on the silicon dioxide surface do not result in SiO_2 dielectric property degradation. Hence, with the citric acid, EWOD reliability is improved relative to NaCl.

The average contact angle at zero voltage for all measurements (eight measurements altogether: four measurements with NaCl and four measurements with citric acid) is also shown in Fig. 5, where the error bars represent the corresponding standard deviation. The consistent contact angle at zero volts shows that there is no contact angle degradation during 10,000 trials. The consistency of the contact angle at zero voltage could be attributed to the fact that Cytop and its hydrophobic properties remain intact during the trials and there is insignificant charge entrapment in the dielectric.

3. Conclusions

In conclusion, voltage drop at the auxiliary electrode is shown to be one source of EW response asymmetry with the applied voltage polarity. Symmetric electrowetting is observed with Si/SiO_2/Cytop substrates, which is attributed to the absence of electrochemical reactions in the auxiliary electrode. Additionally, reliable electrowetting is achieved with thermally grown SiO_2 layers. SiO_2 thermal growth and Cytop coating are the only fabrication steps, which are standard and cost-effective. Lab-on-a-chip devices would benefit from this simple and stable electrowetting system.

Acknowledgements

Support for this work was provided by the National Science Foundation through CMMI-113075.

References

[1] T.B. Jones, J. Micromech. Microeng. 15 (2005) 1184.
[2] B.H.W. Hendriks, S. Kuiper, M.A.J. As, C.A. Renders, T.W. Tukker, Opt. Rev. 12 (2005) 255(LA - English).
[3] B.J. Feenstra, R.A. Hayes, R.v. Dijk, R.G.H. Boom, M.M.H. Wagemans, I.G.J. Camps, A. Giraldo, B.v.d. Heijden, 19th IEEE International Conference on MicroElectroMechanical Systems, 2006, p. 48.
[4] T. Krupenkin, J.A. Taylor, Nat. Commun. 2 (2011) 448.
[5] W.C. Nelson, I. Peng, G.-A. Lee, J.A. Loo, R.L. Garrell, C.-J. "Cj" Kim, Anal. Chem. 82 (2010) 9932.
[6] J.L. Poulos, W.C. Nelson, T.-J. Jeon, C.-J. Kim, J.J. Schmidt, Appl. Phys. Lett. 95 (2009) 13706.
[7] W. Satoh, M. Loughran, H. Suzuki, J. Appl. Phys. 96 (2004) 835.
[8] E.R.F. Welch, Y.-Y. Lin, A. Madison, R.B. Fair, Biotechnol. J. 6 (2011) 165.
[9] F. Mugele, J.-C. Baret, J. Phys. Condens. Matter 17 (2005) R705.
[10] S. Chevalliot, S. Kuiper, J. Heikenfeld, J. Adhes. Sci. Technol. 26 (2012) 1909.
[11] E. Seyrat, R.A. Hayes, J. Appl. Phys. 90 (2001) 1383.
[12] M. Khodayari, B. Hahne, N.B. Crane, A.A. Volinsky, Appl. Phys. Lett. 102 (2013) 192907.
[13] A. Schultz, S. Chevalliot, S. Kuiper, J. Heikenfeld, Thin Solid Films 534 (2013) 348.
[14] B. Raj, M. Dhindsa, N.R. Smith, R. Laughlin, J. Heikenfeld, Langmuir 25 (2009) 12387.
[15] M. Khodayari, J. Carballo, N.B. Crane, Mater. Lett. 69 (2012) 96.
[16] R.B. Mason, J. Electrochem. Soc. 102 (1955) 671.
[17] C.W. Nelson, C.M. Lynch, N.B. Crane, Lab Chip 11 (2011) 2149.
[18] N.B. Crane, A.A. Volinsky, P. Mishra, A. Rajgadkar, M. Khodayari, Appl. Phys. Lett. 96 (2010) 104103.
[19] P.D. Lickiss, in: A.G. Sykes (Ed.), Advances in Inorganic Chemistry, vol. 42, Academic Press, 1995, p. 147.
[20] I. Lukes, M. Borbaruah, L.D. Quin, J. Am. Chem. Soc. 116 (1994) 1737.